The antifibrotic effect and mechanism of a novel tyrosine kinase inhibitor, ZSP1603, in preclinical models of pulmonary fibrosis

Z.-W. LIU^{1,2,3}, M.-Y. ZHAO¹, X.-L. SU³, T.-H. YE³, Y.-J. ZHUANG⁴, Y. ZHANG⁵, Z.-Z. ZHANG¹, J.-L. YANG³, L.-J. CHEN³, C.-F. LONG², Y.-Q. YAO^{1,3}, X.-X. CHEN²

Zhuowei Liu and Manyu Zhao contributed equally to this study

Abstract. – OBJECTIVE: This study aimed to investigate the efficacy and molecular mechanisms of ZSP1603 as a novel anti-fibrotic compound.

MATERIALS AND METHODS: The unilateral left pulmonary fibrosis model was established in the Sprague Dawley (SD) rats. The bilateral pulmonary fibrosis model was established in the C57BL/6J mice. The therapeutic treatment regimen began after the induction of pulmonary fibrosis. The preventive treatment regimen began on the first day of bleomycin administration. Animals were randomly divided into the sham, model, Nintedanib, and ZSP1603 treatment groups. Haematoxylin and eosin (H&E) and Masson's trichrome staining were performed to evaluate pulmonary injury, inflammation, and fibrosis. Cell Counting Kit-8 (CCK-8) assay and Western blot were used to investigate the effects and mechanisms of ZSP1603 on the proliferation of primary human pulmonary fibroblasts (pHPFs). The messenger ribonucleic acid (mRNA) expression of transforming growth factor (TGF)-β1, tissue inhibitor of metalloproteinase 1 (TIMP-1), and collagen 1A1 (COL1A1) in pHPFs was detected by quantitative Real Time-Polymerase Chain Reaction (PCR).

RESULTS: ZSP1603 inhibited the proliferation of pHPFs *in vitro* by blocking the platelet-derived growth factor receptor-β (PDGF-Rβ) and extracellular signal-regulated kinase (ERK) signalling pathway. ZSP1603 also inhibited the differentiation of pHPFs by reducing the expression of TGF-β1, TIMP-1, and COL1A1. ZSP1603 significantly attenuated pulmonary injury, inflammation, and fibrosis *in vivo* in four independent animal studies of pulmonary fibrosis.

CONCLUSIONS: ZSP1603 is an effective anti-fibrotic compound with clear mechanisms.

Key Words:

Tyrosine kinase inhibitor, Idiopathic pulmonary fibrosis, PDGFRβ, Anti-fibrotic drug, Anti-inflammatory.

Introduction

Idiopathic pulmonary fibrosis (IPF) is a fibrotic interstitial pneumonia with an irreversible decline in lung function and high mortality¹⁻³. The incidence of IPF has recently increased, especially in older adults³⁻⁵.

Although the pathogenic mechanisms were not fully understood, the understanding of IPF has evolved over the years. Injury, inflammation, and repair are the major stages of pulmonary fibrosis⁶. Various factors, including environmental particulate matter, allergens, and infectious agents, may lead to lung injury. Injuries to the bronchioles, arterioles, and alveolar epithelia initiate wound healing response, where immune cells and fibroblasts are recruited⁷. Sustained pulmonary injury leads to excess release of inflammatory factors, chemotactic factors, and profibrotic cytokines, such as PDGFs, TGF-β, vascular endothelial growth factors (VEGFs), fibroblast growth factors (FGFs), matrix metalloproteinases (MMPs), and TIMPs⁸. Profibrotic cytokines promote fibroblast proliferation and stimulate the differentiation of fibroblasts into myofibroblasts. The excessive deposition of extracellular matrix (ECM) induced

¹West China School of Public Health and West China Fourth Hospital, Healthy Food Evaluation Research Center, Sichuan University, Chengdu, China

²Guangdong Raynovent Biotech Co., Ltd. Guangdong, China

³State Key Laboratory of Biotherapy and Cancer Center, West China Hospital, Sichuan University, Chengdu, China

⁴KCI Biotech Inc., Suzhou, China

⁵WuXi AppTec Ltd., Shanghai, China

by activated fibroblasts and myofibroblasts causes pulmonary fibrosis⁹. Some aberrant growth factor signals, such as PDGF/PDGFRs, VEGF/VEGFRs, and FGF/FGFRs, are the major pathogenic factors in the pathogenesis. Tyrosine kinase inhibitors (such as Nintedanib and Lenvatinib) suppressing fibroblast proliferation and differentiation are effective for pulmonary fibrosis¹⁰⁻¹².

ZSP1603, designed and synthesized in our lab, is a novel selective triple tyrosine kinase inhibitor that mainly targets PDGFRs, FGFRs, and VEG-FRs¹³⁻¹⁵. The molecular structure of ZSP1603 was shown in Figure 1A and the target kinases were presented in *Supplementary Table I*. However, the mechanisms of ZSP1603 as an anti-fibrotic compound have not been fully understood. In this study, we analysed its effects and molecular mechanisms in pulmonary fibrosis therapy.

Materials and Methods

Cell Culture

pHPFs were obtained from the ScienCell Research Laboratories, Inc. (Carlsbad, CA, USA). The pHPFs were cultured in Fibroblast Medium (FM, Cat: 2301, ScienCell, Carlsbad, CA, USA) and maintained in a cell incubator at 37°C with 5% CO₂. The cells were allowed to grow into 90% confluence before the experiments¹⁶.

Assay of pHPFs Proliferation

The effects of ZSP1603 on the proliferation of pHPFs were detected by Cell Counting Kit-8 (CCK-8) assay¹⁷. Briefly, the tenth-generation cells were seeded in 96-well plates (1×10⁴ cells per well). After starving overnight, the cells were treated with a series of different concentrations of ZSP1603 (0-25 μΜ) and 50 ng/mL human PDGF-BB. 48 h later, CCK-8 solution (ZETA-LIFE, Menlo Park, CA, USA) was added to the cell culture medium and incubated for other 4 h at 37°C. The absorbance was measured at 450 nm using a microplate reader (Synergy HT, Bio-Tek, Winooski, VT, USA)¹⁸.

Western Blot

After cultivation in serum-free medium for 24 h, the cells were incubated with ZSP1603 (0, 0.5, 5.0, and 50.0 μ M) for 4 h and subsequently stimulated with PDGF-BB (50 ng/mL) for 15 minutes. Then, the cells were lysed in Radio Immunoprecipitation Assay (RIPA) lysis buffer (Biosharp, Hefei, Anhui, China) containing

protease inhibitors (Beyotime, Shanghai, China) and phosphatase inhibitors (MedChemExpress, Middlesex, NJ, USA). The protein concentrations were determined by the Bicinchoninic acid (BCA) assay (Beyotime, Shanghai, China). The protein lysates were electrophoretically separated on 10% SDS-PAGE gels and transferred to polyvinylidene difluoride (PVDF) membranes. After blocking with 5% skimmed milk for 2 h, the membranes were incubated with antibodies against phospho-PDGFRB (Tyr751, Cell Signaling Technology, Danvers, MA, USA), PDG-FRB (Cell Signaling Technology, Danvers, MA, USA), phospho-ERK1/2 (pERK1/2, Thr202/ Tyr204, HuaAn Biotechnology, Hangzhou, Zhejiang, China), ERK1/2 (HuaAn Biotechnology, Hangzhou, Zhejiang, China), and β-actin (HuaAn Biotechnology, Hangzhou, Zhejiang, China) at 4°C overnight. Then, the membranes were incubated with secondary antibodies for 1 h. The blots were visualized using ChemiDocTM XRS + System with Image LabTM Software (Bio-Rad Laboratories, Inc., Hercules, CA, USA). The relative signal intensity of each band was determined by Image J analysis software. β-actin was used as the loading control¹⁹.

Quantitative Real-time Polymerase Chain Reaction

Gene expression was quantified by SYBR green Real Time Polymerase Chain Reaction (RT-PCR) on a Stratagene Mx3005 System (Agilent Technologies, Santa Clara, CA, USA). β-actin was used as an internal control. The relative gene expression compared with control group 2 (stimulated with PDGF-BB without ZSP1603 or Nintedanib) was calculated²⁰. The primer sequences were listed in *Supplementary Table II*.

Establishment of the Bleomycin-induced Pulmonary Fibrosis Model in Animals

The animal experiments were approved by the Institutional Animal Care and Treatment Committee of KCI Biotech Inc. (Suzhou, Jiangsu, China, No. 2016022, 1 April 2016). For bleomycin-induced unilateral left pulmonary fibrosis models in Sprague Dawley (SD) rats, bleomycin (3 mg/kg) was administrated through a PE20 catheter intubating to the left pulmonary bronchus. For bilateral pulmonary fibrosis models in male C57BL/6J mice, bleomycin (2.5 mg/kg) was administrated intratracheally²¹. The study designs were shown in Table I.

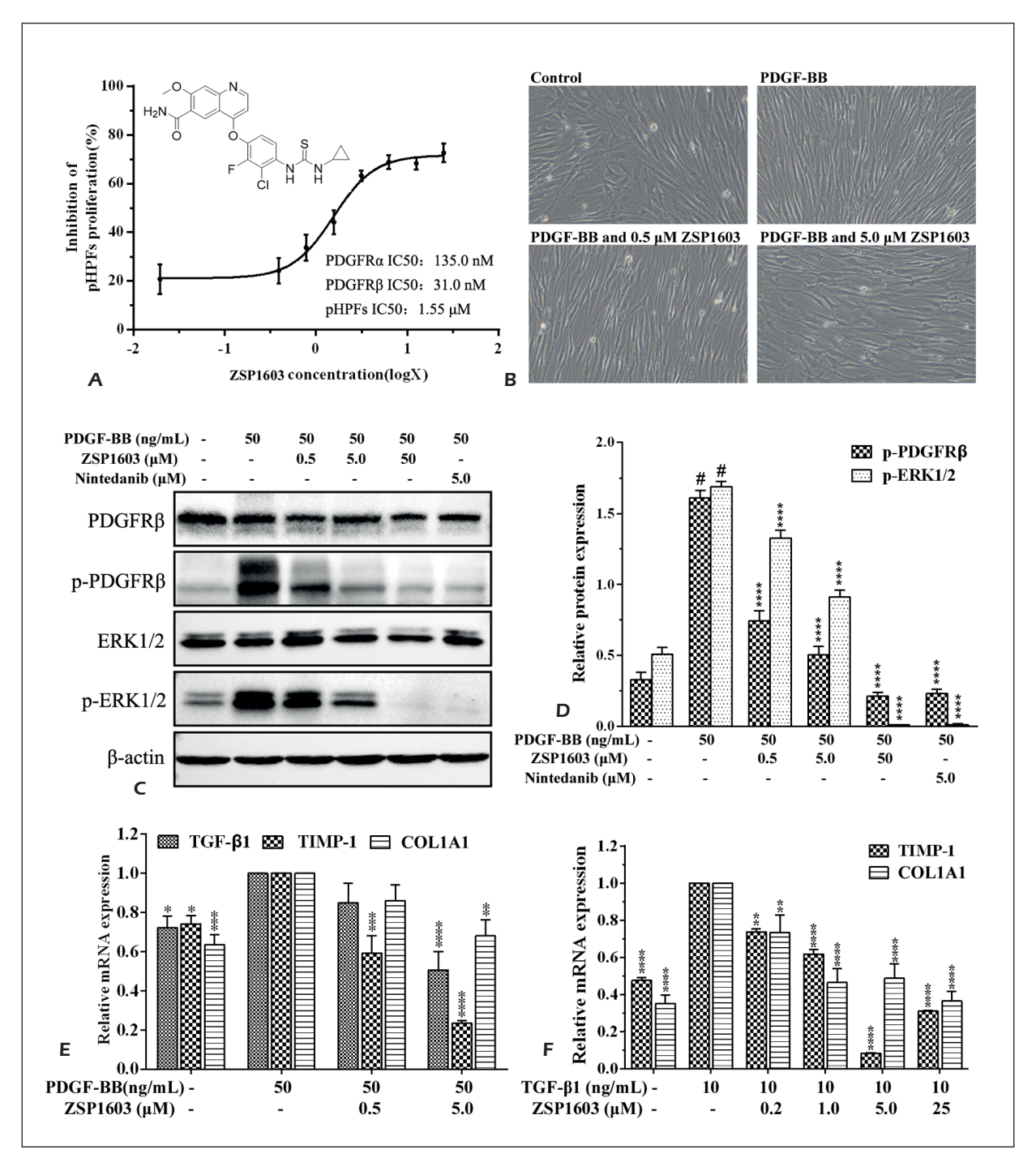


Figure 1. ZSP1603 inhibited the proliferation and differentiation of pulmonary fibroblasts. **A**, Molecular structure of ZSP1603 and its effect on inhibiting the proliferation of pHPFs. **B**, Images showing the typical morphology of pHPFs in each group (400×). **C**, Western blot showing the levels of the total and phosphorylated PDGFR and ERK1/2 proteins in pHPFs. **D**, Statistical analysis of the data presented in C (*p<0.0001 compared with the PDGF-BB-free group; ****p<0.001 compared with the PDGF-BB control group). **E**, ZSP1603 reduced the mRNA expression of TGF-β1, TIMP-1 and COL1A1 in pHPFs stimulated with PDGF-BB. **F**, ZSP1603 reduced the mRNA expression of TIMP-1 and COL1A1 in pHPFs stimulated with TGF-β1. *p<0.05, **p<0.01, ***p<0.001 and ****p<0.0001.

Study designs	Unilateral left pulmonary fibrosis model in rat		Bilateral pulmonary fibrosis model in mice	
	Preventive	Therapeutic	Preventive	Therapeutic
ZSP1603 groups (mg/kg/day)	25, 100, 200	50, 100	25, 50, 100	25, 50, 100
Nintedanib control groups (mg/kg/day)	100	50, 100	50	50
Study duration (day)	14	21	14	21
Duration of medication (day)	1 th -14 th	8 th -21 th	1 th -14 th	8 th -21 th

Table I. Study designs of ZSP1603 in bleomycin induced pulmonary fibrosis models.

Histology

Haematoxylin and eosin (H&E) staining and Masson's trichrome staining were performed to evaluate pulmonary injury, inflammation, and fibrosis²². After staining, an image of the whole lung was captured for further pathological analysis. The evaluation criteria for pulmonary injury and inflammation were shown in *Supplementary Table III*. Masson's trichrome staining was used to evaluate the extent of pulmonary fibrosis according to the Ashcroft scoring protocols²³.

Statistical Analysis

The data were presented as the mean \pm Standard Error of Mean (SEM). The results were analysed either with One-way analysis of variance (ANOVA) followed by Dunnett's post-hoc test or two-way ANOVA followed by Bonferroni's post-hoc test (GraphPad Prism 6.0, La Jolla, CA, USA). p<0.05 was considered significant.

Results

ZSP1603 Inhibited the Proliferation of Pulmonary Fibroblasts

The results of the CCK-8 assay showed that ZSP1603 inhibited the proliferation of pHPFs induced by PDGF-BB (50 ng/mL). The IC $_{50}$ value was 1.55±0.19 μ M (Figure 1A). Representative images of pHPFs were shown in Figure 1B.

ZSP1603 Inhibited the Phosphorylation of PDGFR and ERK1/2 in Pulmonary Fibroblasts

To explore the molecular mechanism of ZSP1603 on the proliferation of pHPFs, Western blot was used to evaluate the expression of PDGFR β and its downstream ERK1/2. The experimental groups were shown in Figure 1C. After 4 h of treatment with ZSP1603 or Nintedanib, pHPFs were stimulated with 50 ng/mL PDGF-BB

for 15 minutes. PDGF-BB increased the phosphorylation of PDGFR β and ERK1/2 in pHPFs (p<0.0001). The phosphorylation of PDGFR β and ERK1/2 was significantly inhibited by ZSP1603 in a dose-dependent manner compared with the PDGF-BB control group (p<0.0001, Figure 1D).

ZSP1603 Inhibited the Differentiation of Pulmonary Fibroblasts by Reducing the Expression of TGF- β 1, TIMP-1, and COL1A1 in pHPFs

Quantitative Real Time-PCR was used to detect the expression of genes associated with fibrosis in pHPFs stimulated by PDGF-BB and TGF-β1. 50 ng/mL PDGF-BB treatment upregulated the mRNA expression of TGF-β1, TIMP-1, and CO-L1A1 (TGF- β 1 and TIMP-1, p<0.05; COL1A1, p<0.001) (Figure 1E), but these effects were inhibited by co-treatment with ZSP1603 (Figure 1E). TIMP-1 and COL1A1 were upregulated by 10 ng/ mL TGF- β 1 (p<0.0001) and these changes were inhibited by ZSP1603 (Figure 1F). The increased mRNA expression of α-SMA in pHPFs induced by 20 ng/mL TGF-β1 was also suppressed by ZSP1603 (Supplementary Figure 1). Typical images of pHPFs in each group treated with 20 ng/mL TGF-β1 were shown in *Supplementary Figure 2*.

ZSP1603 Attenuated Pulmonary Injury, Inflammation and Fibrosis in Bleomycin-induced Pulmonary Fibrosis Model of Rats

The study designs were shown in Table I. In the therapeutic regimen experiment, the body weight of rats in each group decreased in the first five days and began to recover on the sixth day (Figure 2A). The left lung weight of rats in the bleomycin treatment group was lower than that of rats in the sham operation group (Figure 2B, p<0.001).

H&E and Masson's trichrome staining of whole left lung tissues were performed to evaluate pulmonary injury, inflammation, and fibro-

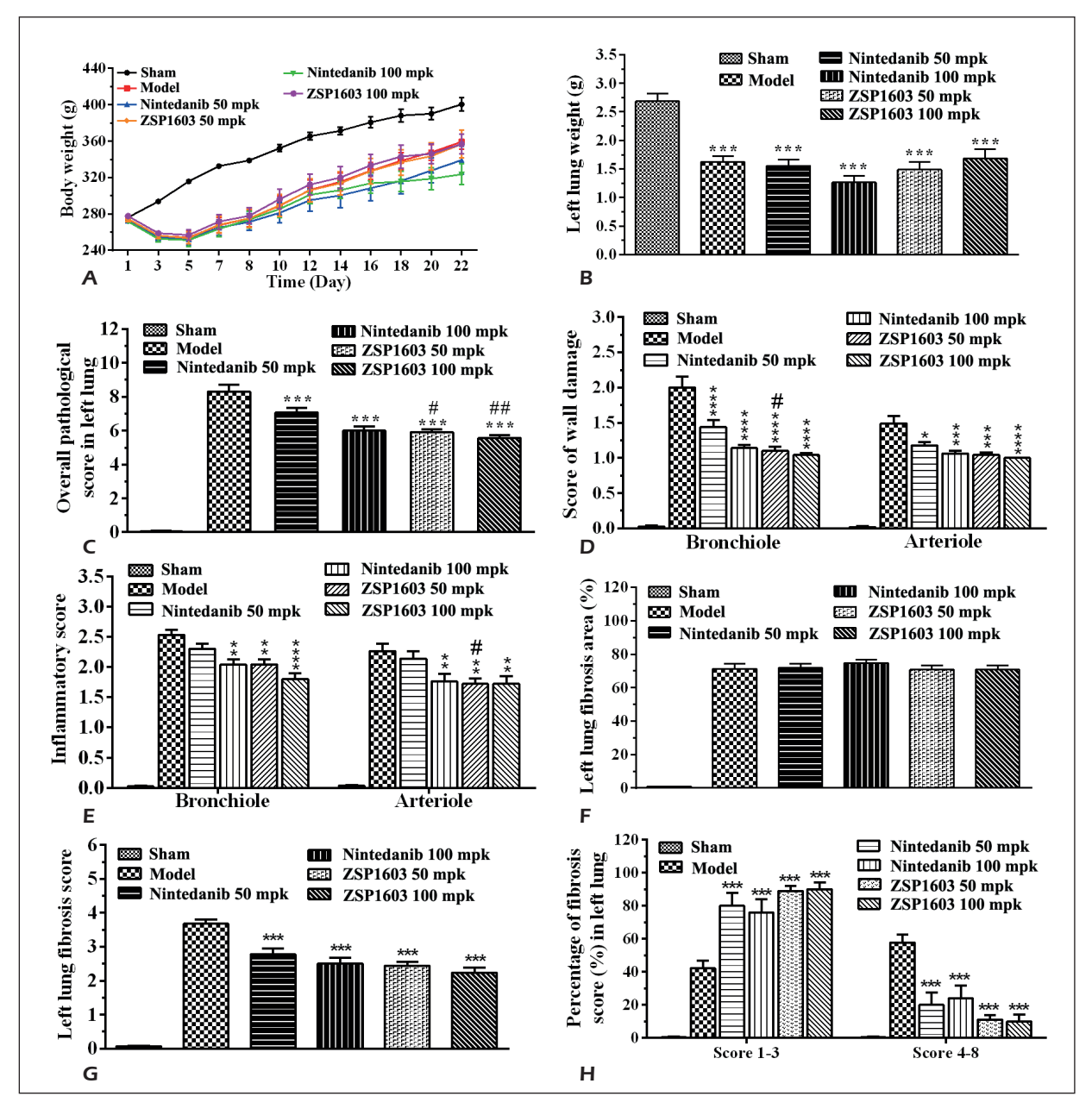


Figure 2. Therapeutic effect of ZSP1603 on the rat model of bleomycin-induced unilateral left pulmonary fibrosis. **A**, Changes in the body weight of rats in each group. **B**, Weight of the left lungs in each group. **C**, The overall pulmonary pathological score, including wall damage and the inflammation of the bronchioles and arterioles. **D**, The pathological score for pulmonary damage in the bronchiole and arteriole walls. **E**, The pathological score for pulmonary inflammation in the bronchioles and arterioles. **F**, The fibrotic area of the left lung. **G**, The fibrosis score of the left lung. **H**, The percentages of animals with fibrosis scores of 1-3 and 4-8 in each group. $^{\#}p<0.05$ and $^{\#\#}p<0.01$ compared with the 50 mpk Nintedanib group; $^{\#}p<0.05$, $^{**}p<0.01$, $^{***}p<0.001$, and $^{***}p<0.0001$ compared with the model group; mpk indicated mg/kg.

sis (Supplementary Figure 3). The standards of pathological evaluation based on H&E staining were shown in Supplementary Table III. The weight, overall pulmonary damage and inflammation score, fibrosis area and fibrosis scores of the left lungs were presented in Supplementa-

ry Table IV and Figure 2C-2H. After treatment with ZSP1603 and Nintedanib, pulmonary injury and inflammation were reduced compared with the model group (p<0.001, Figure 2C-2E). Also, the 50 mpk (mg/kg) ZSP1603 was more effective than the 50 mpk Nintedanib treatment (p<0.05).

Typical images of the criteria used to evaluate pulmonary fibrosis with the Ashcroft scale (0-8 points) were shown in the Supplementary Figure 4. Notably, 70.8-71.9% of the left lungs treated with bleomycin exhibited fibrosis and the areas were not statistically different among the groups (Figure 2F and *Supplementary Table IV*). In the model group, 57.8% of the animals had fibrosis score \geq 4 (Figure 2H). The normal structures of the bronchioles, arterioles, and alveoli were destroyed. Numerous inflammatory cells infiltrated into the lung tissues of the model group (Figure 3A and 3B). The bleomycin-induced damage and inflammatory cell infiltration in the bronchioles, arterioles, and alveoli were significantly reduced by ZSP1603 (Figure 3A and 3B).

After scoring by three qualified pathologists, the fibrosis scores of the left lung were 0, 3.7 ± 0.1 , 2.8 ± 0.2 , 2.5 ± 0.2 , 2.4 ± 0.1 , and 2.2 ± 0.1 for the control, model, 50 mpk Nintedanib, 100 mpk Nin-

tedanib, 50 mpk ZSP1603 and 100 mpk ZSP1603 groups, respectively. ZSP1603 and Nintedanib exerted significant antifibrotic effects (p<0.001, Figures 2G, 3C, and 3D). The pathological scores in the ZSP1603 and Nintedanib treatment groups were significantly decreased compared with the model group (p<0.001, Supplementary Table IV).

In the preventive regimen, the weight of rats at the end of the treatment were 335.6 ± 6.6 , 273.6 ± 8.7 , 261.8 ± 8.7 , 294.5 ± 10.38 , 266.3 ± 12.5 and 281.9 ± 7.1 g in the sham, model, 100 mpk Nintedanib, and ZSP1603 (25, 100 and 200 mpk) groups, respectively. The weight recovery of rats in all ZSP1603 treatment groups were better than 100 mpk Nintedanib group (Figure 4A). Similar results were observed on the left lung weights of mice (*Supplementary Table V*). ZSP1603 reduced pulmonary injury, inflammation, and fibrosis compared with the model group (Figure 4B and 4C). In addition, the pathological score

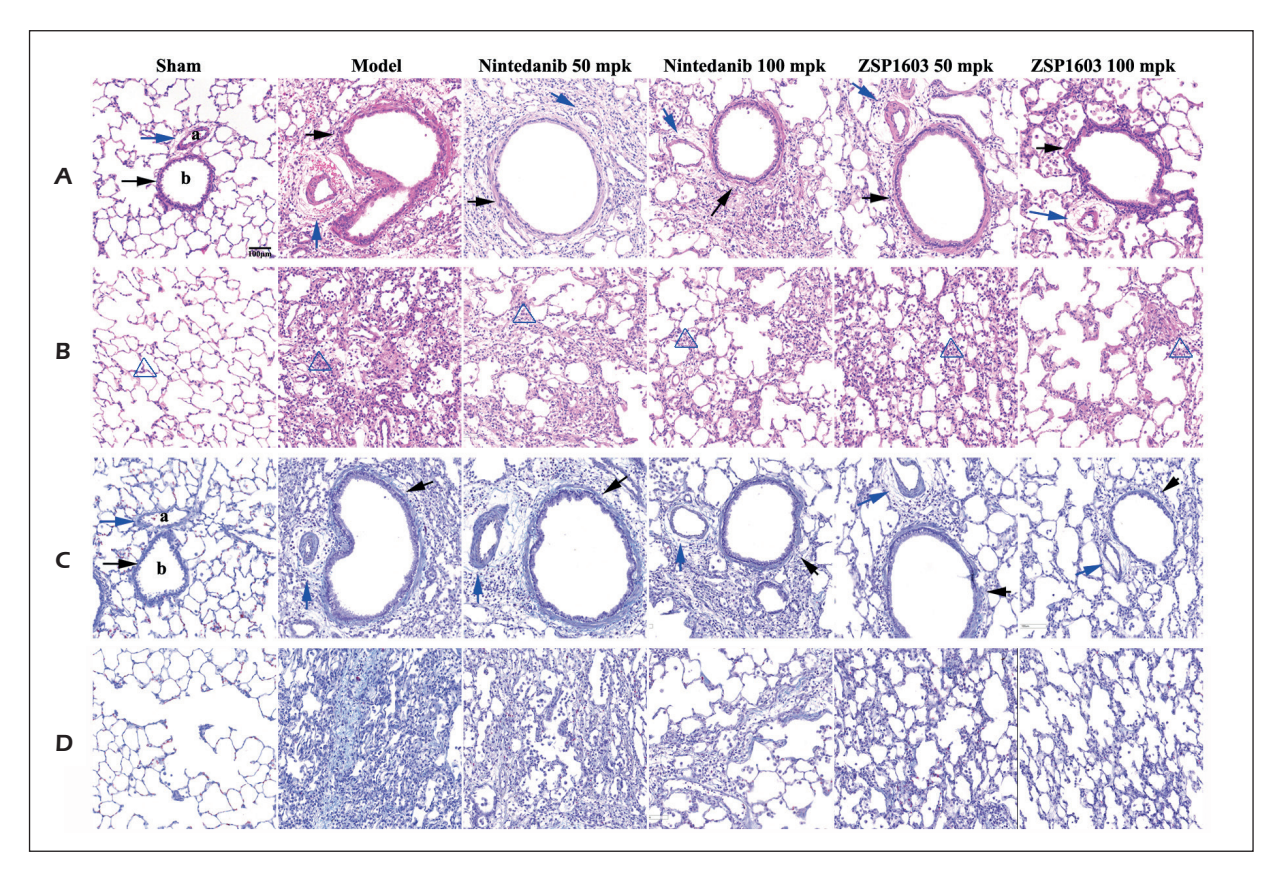


Figure 3. Histological changes in the pulmonary bronchioles, small arteries and alveoli in rats subjected to bleomycin-induced unilateral left pulmonary fibrosis. **A**, Typical histological images of pulmonary bronchioles and small arteries stained with H&E in each group. **B**, Typical images of Masson's trichrome staining in the pulmonary bronchioles and small arteries of each group. **C**, Typical images of H&E staining in the pulmonary alveoli of each group. **D**, Typical images of Masson's trichrome staining in the pulmonary alveoli from each group. a, pulmonary arteries; b, pulmonary bronchioles; blue arrow, the walls of the pulmonary arteries; black arrow, the walls of the pulmonary bronchioles; blue triangle, the alveolar structure; mpk indicated mg/kg. All images were captured by 200× magnification.

of 100 mpk ZSP1603 group was lower than the Nintedanib group (Figure 4C). As shown in the typical images of gross lung pathology presented in Figure 4D, the atrophy of left lung fibrosis induced by bleomycin was worse than that of the right lung in rats. Images of Masson's trichrome staining of the pulmonary alveoli in each group were shown in *Supplementary Figure 5*.

The Therapeutic and Preventive Effects of ZSP1603 on the Mouse Model of Bleomycin-induced Pulmonary Injury and Fibrosis

The body weight of mice in each group was shown in Figure 5A. In the ZSP1603 therapeutic regimen, the gross pathological morphology of lungs in each group was shown in Figure 5B. The overall pathological scores were 0, 7.1±0.3, 5.2±0.3, 6.3±0.3, 5.1±0.1, 4.9±0.2 for the sham group, model group, 50 mpk Nintedanib group, and the three ZSP1603 treatment groups (Figure 5C). ZSP1603 reduced the pulmonary injury and inflammation induced by bleomycin (Figure 5D and *Supplementary Figure 6*). The fibrosis

scores were shown in Figure 5E and *Supplementary Table VI*. Typical images of Masson's trichrome staining were shown in Figure 5F and *Supplementary Figure 7*. These results indicated that ZSP1603 had promising anti-fibrotic effects. The results of preventive studies also confirmed that ZSP1603 attenuated bleomycin-induced lung injury (Figure 6A and 6D), inflammation (Figure 6B and 6D), and fibrosis (Figure 6C and 6D) *in vivo* (*Supplementary Figures 8-10* and *Supplementary Table VII*).

Discussion

IPF is a progressive disease with a median survival of 3 to 5 years after diagnosis. Nintedanib, a tyrosine kinase inhibitor, exhibits significant clinical benefits in patients with IPF. In this study, using human pulmonary fibroblasts and different preclinical models of pulmonary fibrosis, we demonstrated that ZSP1603, which targets multiple receptors of tyrosine kinases, is a potential therapeutic small molecular drug for IPF.

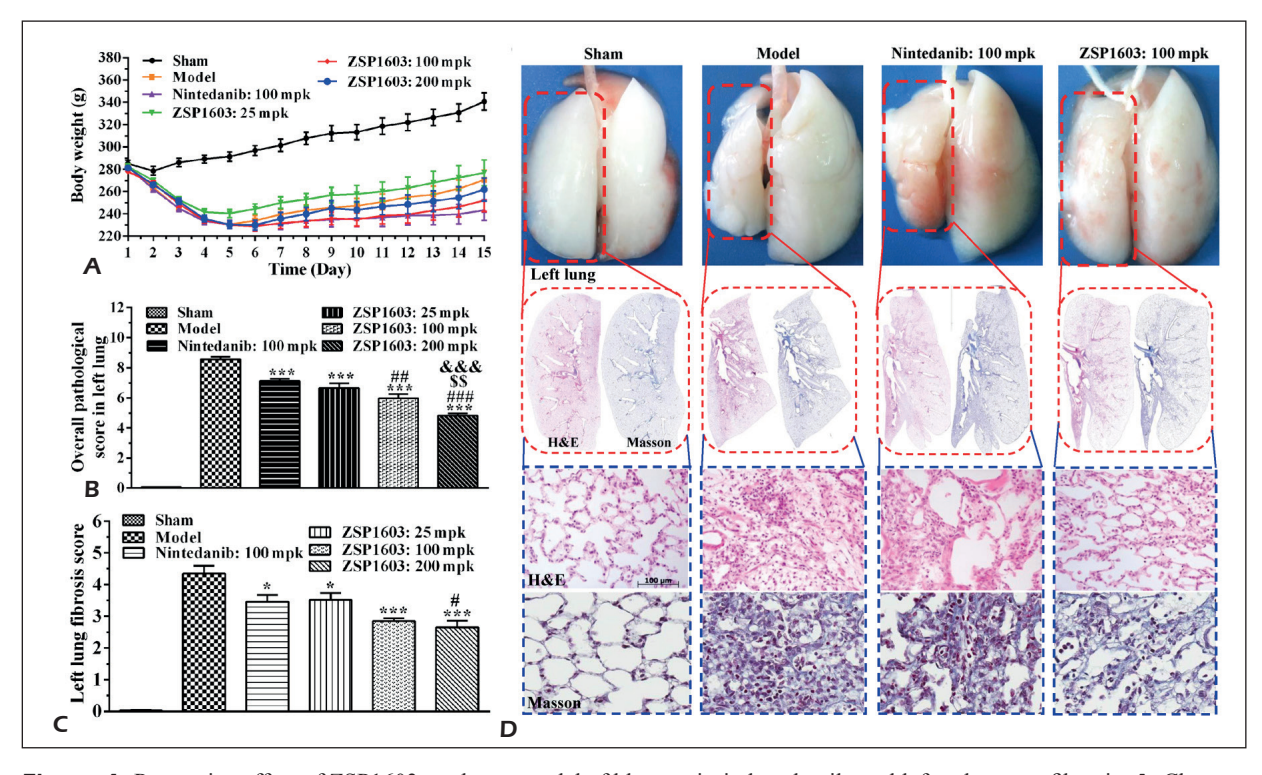


Figure 4. Preventive effect of ZSP1603 on the rat model of bleomycin-induced unilateral left pulmonary fibrosis. **A**, Changes in the body weight of rats in each group. **B**, Statistics for the overall pulmonary pathological score of each group. **C**, The fibrosis score of the left lung. **D**, The gross pathological changes in morphology and histology in the left lung of rats in each group (magnification: $200\times$). **p<0.05, ***p<0.01 and ****p<0.01 compared with the Nintedanib control group; **p<0.01 compared with the 25 mpk ZSP1603 group; **p<0.01 compared with the 100 mpk ZSP1603 group; **p<0.01, ***p<0.01, and ****p<0.001 compared with the model group; mpk indicated mg/kg.

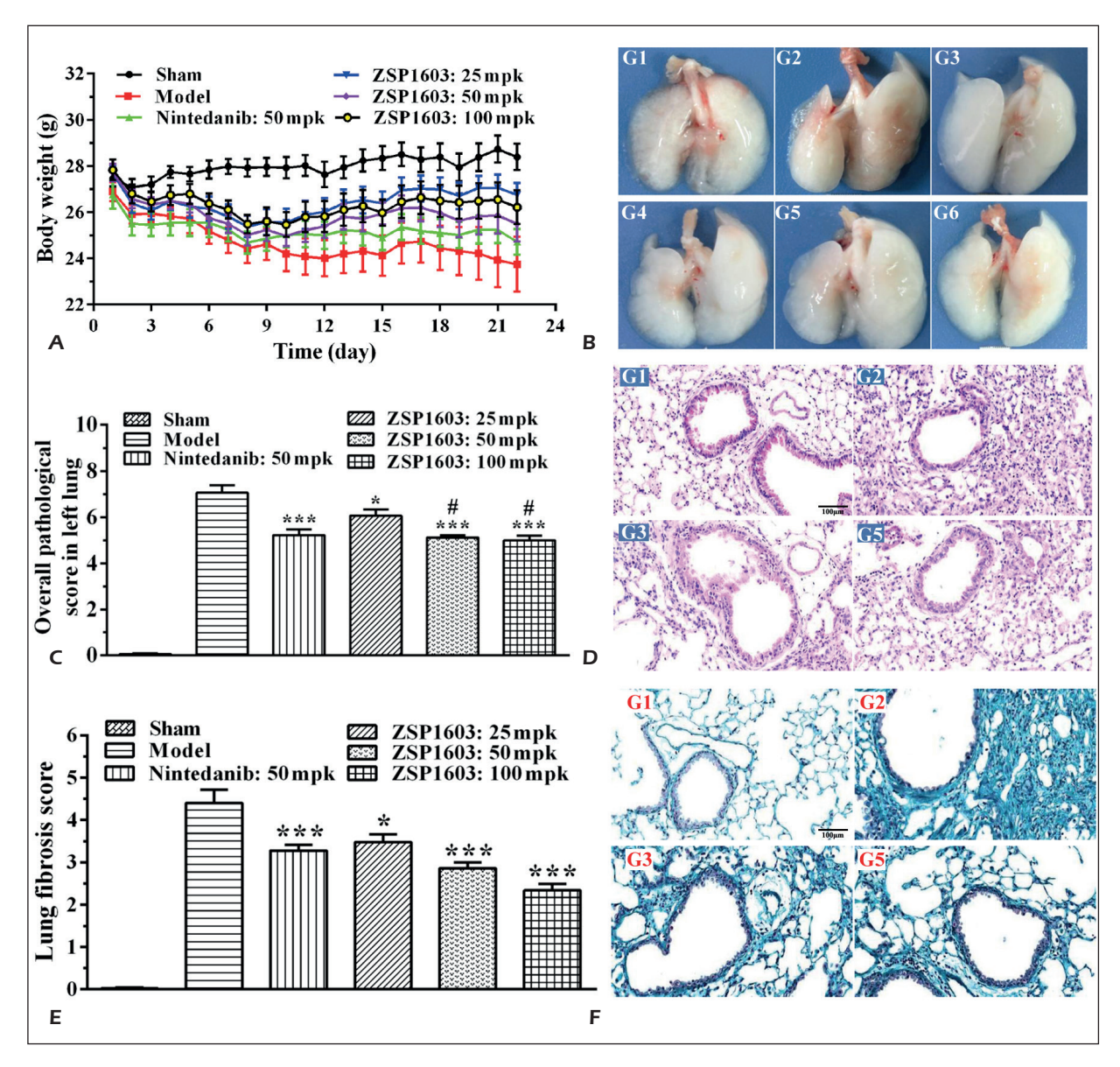


Figure 5. Therapeutic effects of ZSP1603 on pulmonary injury, inflammation and fibrosis in the mouse model of bleomycin-induced pulmonary injury and fibrosis. **A**, Changes in the body weight of mice in each group. **B**, The gross pathological morphology of the lungs in each group. **C**, The statistics for the overall pulmonary pathological scores of each group. **D**, The histological changes in the bronchioles, arteriole walls and alveoli of the lungs (H&E staining, magnification: 200^{\times}). **E**, The fibrosis score in each group. **F**, The histological changes in the lungs (Masson staining, magnification: 200^{\times}). $^{\#}p<0.05$ compared with the 50 mpk Nintedanib group; $^{*}p<0.05$ and $^{**}p<0.001$ compared with the model group; mpk indicated mg/kg. G1: sham; G2: model; G3: 50 mg/kg/day Nintedanib; G4: 25 mg/kg/day ZSP1603; G5: 50 mg/kg/day ZSP1603.

The malignant proliferation and differentiation of pulmonary fibroblasts lead to excessive accumulation of ECM and promotes pulmonary fibrosis in patients with IPF²⁴. PDGF-BB is a profibrotic cytokine that activates the mitotic signalling pathway of fibroblasts, such as the ERK downstream signalling pathway. PDGF-BB/PDGFR/ERK1/2 is a major pathogenic pathway

in IPF. Upon stimulation with PDGF-BB, pHPFs exhibited a substantial increase in proliferation. According to the results of the proliferation assay, ZSP1603 significantly inhibited the PDGF-BB-induced proliferation of pHPFs. Western blot results showed that ZSP1603 inhibited fibroblast proliferation by suppressing the PDGF-BB/PDGFRβ/ERK1/2 signalling pathway.

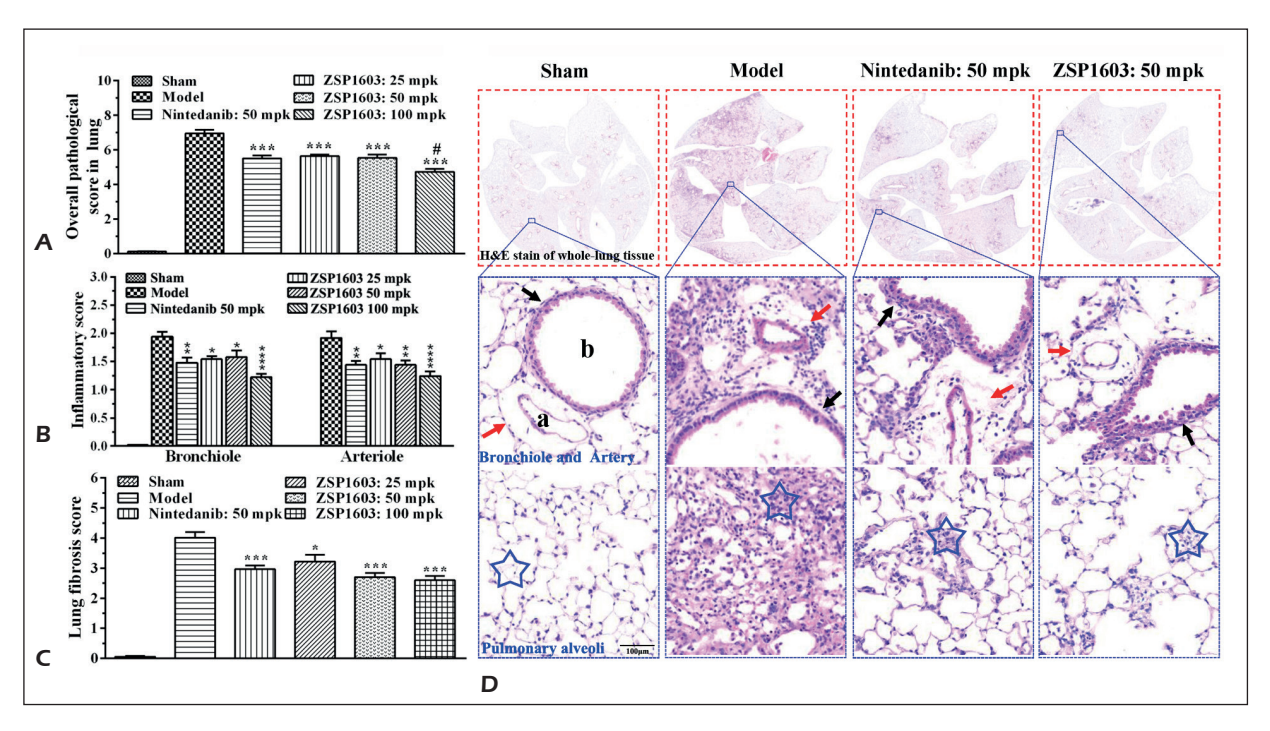


Figure 6. Preventive effects ZSP1603 on pulmonary injury, inflammation and fibrosis in the mouse model of bleomycin-induced pulmonary injury and fibrosis. **A**, Overall pulmonary pathological scores of each group. **B**, The pathological score for pulmonary inflammation in the bronchioles and arterioles. **C**, The fibrosis score in each group. **D**, Typical images of whole lungs, pathological sections and histological changes in pulmonary injury and inflammation in the pulmonary bronchioles, small arteries and alveoli areas were shown (magnification: $200 \times$). The red arrow indicates the walls of the pulmonary arteries, the black arrow indicated the walls of the pulmonary bronchioles, and the blue five-pointed star indicated the inflammatory cell infiltration in alveolar areas. *p<0.05 compared with the 50 mpk Nintedanib group; *p<0.05, **p<0.01, ***p<0.001, and ****p<0.0001 compared with the model group; mpk indicated mg/kg.

TGF-β1, which drives fibroblasts to differentiate into myofibroblasts, is a vital profibrotic cytokine in pulmonary fibrosis²⁵. Activated myofibroblasts secrete ECM components, such as collagens, and promote pulmonary fibrosis. TIMP-1 is overexpressed in activated fibroblasts and exerts multiple stimulatory effects on the development and progression of pulmonary fibrosis. As an endogenous inhibitor of metalloproteinases, TIMP-1 induces fibroblast differentiation and inhibits the apoptosis of myofibroblasts in fibrotic tissues²⁶. In addition, TIMP-1 promotes fibrosis by inhibiting MMP-mediated ECM degradation²⁷. Both TGF-β1 and TIMP-1 are highly expressed in patients with IPF. In the present study, ZSP1603 significantly decreased the expression of TGF-β1, TIMP-1, and COL1A1 in pHPFs stimulated with PDGF-BB. Besides, ZSP1603 also suppressed the expression of TIMP-1, COL1A1, and α-SMA in pHPFs stimulated with TGF-β1. Based on these findings, we infer that ZSP1603 can inhibit the differentiation of fibroblasts into myofibroblasts

by inhibiting the upregulation of TGF- β 1, TIMP-1, COL1A1, and α -SMA induced by PDGF-BB.

The therapeutic and preventive effects of ZSP1603 on pulmonary injury, inflammation, and fibrosis were explored in the rats and mice models of bleomycin-induced pulmonary fibrosis. No death occurred in the bleomycin-induced unilateral left pulmonary fibrosis model during the study. Moreover, some advantages of ZSP1603 were observed compared with Nintedanib. As shown in Figure 2, the suppressive effects of ZSP1603 (50 mpk group in the therapeutic study) on pulmonary injury (bronchioles) and inflammation (arterioles) were more effective than that of Nintedanib in the same dose in the rat fibrosis model. Meanwhile, ZSP1603 was more tolerant and safer than Nintedanib based on the observed changes in body weight. The respiratory functions and lung hydroxyproline levels treated with ZSP1603 and Nintedanib were not significantly different compared to the control group (Supplementary Figures 11-12).

Conclusions

ZSP1603 is an effective anti-fibrotic compound for pulmonary fibrosis therapy, with clear molecular mechanisms and therapeutic effects in preclinical animal models.

Author Contributions

Yuqin Yao and Xiaoxin Chen designed this research. Zhuowei Liu and Manyu Zhao performed most of the experiments. Xiaolan Su and Tinghong Ye instructed some experiments. Yongjie Zhuang and Yang Zhang collected and interpreted data. Yuqin Yao and Manyu Zhao wrote this paper. Zunzhen Zhang revised the paper. Yuqin Yao, Jinliang Yang, Lijuan Chen, and Chaofeng Long were responsible for fund collection and revised this paper.

Acknowledgments

This study was funded by the National Natural Science Foundation of China (No. 81773375) and the National Major Scientific and Technological Special Project (2018ZX09201002, 2018ZX09711001-011 and 2019ZX09201001). The authors thank the research platform provided by Public Health and Preventive Medicine Provincial Experiment Teaching Center of Sichuan University, Food Safety Monitoring and Risk Assessment Key Laboratory of Sichuan Province.

Conflict of Interests

All the authors declare that they have no conflict of interests. All the institutions and companies declare that they have no conflict of interests. In this study, ZSP1603 was provided by Guangdong Raynovent Biotechnology Co., Ltd. Sichuan University, including State Key Laboratory of Biotherapy and Cancer Center, West China School of Public Health and West China Fourth Hospital, provided platforms for performing the experiments. KCI Biotech Inc. and WuXi AppTec Ltd. provided assistance for animal experiments in this study.

Zhuowei Liu, Xiaoxin Chen, and Chaofeng Long are employees of Guangdong Raynovent Biotechnology Co., Ltd. Zhuowei Liu is an on-the-job Ph.D student of Sichuan University. Yongjie Zhuang is an employee of KCI Biotech Inc. Yang Zhang is an employee of WuXi AppTec Ltd. The other authors, all from Sichuan University, participated in the study.

References

- 1) LEDERER DJ, MARTINEZ FJ. Idiopathic pulmonary fibrosis. N Engl J Med 2018; 378: 1811-1823.
- 2) GEORGE PM, PATTERSON CM, REED AK, THILLAI M. Lung transplantation for idiopathic pulmonary fibrosis. Lancet Respir Med 2019; 7: 271-282.
- 3) KROPSKI JA, BLACKWELL TS. Progress in understanding and treating idiopathic pulmonary fibrosis. Annu Rev Med 2019; 70: 211-224.
- 4) Novelli F, Tavanti L, Cini S, Aouilini F, Melosini L, Romei C, Sbragia P, Falaschi F, Celi A, Paggiaro P. Determi-

- nants of the prognosis of idiopathic pulmonary fibrosis. Eur Rev Med Pharmacol Sci 2014; 18: 880-886.
- CARBONE R, BALLEARI E, GROSSO M, MONTANARO F, BOTTINO G, GHIO R. Predictors of mortality of idiopathic pulmonary fibrosis. Eur Rev Med Pharmacol Sci 2008; 12: 97-104.
- 6) GOODWIN AT, JENKINS G. Molecular endotyping of pulmonary fibrosis. Chest 2016; 149: 228-237.
- WILSON MS, WYNN TA. Pulmonary fibrosis: pathogenesis, etiology and regulation. Mucosal Immunol 2009; 2: 103-121.
- Qiu Y, PAN X, Hu Y. Polydatin ameliorates pulmonary fibrosis by suppressing inflammation and the epithelial mesenchymal transition via inhibiting the TGF-β/Smad signalling pathway. RSC Adv 2019; 9: 8104-8112.
- KADLER KE, HILL A, CANTY-LAIRD EG. Collagen fibrillogenesis: fibronectin, integrins, and minor collagens as organizers and nucleators. Curr Opin Cell Biol 2008; 20: 495-501.
- 10) RICHELDI L, DU BOIS RM, RAGHU G, AZUMA A, BROWN KK, COSTABEL U, COTTIN V, FLAHERTY KR, HANSELL DM, INOUE Y, KIM DS, KOLB M, NICHOLSON AG, NOBLE PW, SELMAN M, TANIGUCHI H, BRUN M, LE MAULF F, GIRARD M, STOWASSER S, SCHLENKER-HERCEG R, DISSE B, COLLARD HR, Investigators IT. Efficacy and safety of Nintedanib in idiopathic pulmonary fibrosis. N Engl J Med 2014; 370: 2071-2082.
- 11) EISEN T, SHPARYK Y, MACLEOD N, JONES R, WALLENSTEIN G, TEMPLE G, KHDER Y, DALLINGER C, STUDENY M, LOEM-BE AB, BONDARENKO I. Effect of small angiokinase inhibitor Nintedanib (BIBF 1120) on QT interval in patients with previously untreated, advanced renal cell cancer in an open-label, phase II study. Invest New Drugs 2013; 31: 1283-1293.
- 12) Collery P, Veena V, Harikrishnan A, Desmaele D. The rhenium(I)-diselenoether anticancer drug targets ROS, TGF-beta1, VEGF-A, and IGF-1 in an in vitro experimental model of triple-negative breast cancers. Invest New Drugs 2019 37: 973-983.
- 13) Long C, Chen Z, Chen X, Zhang Y, Liu Z, Chen S, Chen L, Yang J, Qian Z. Application of tyrosine kinase inhibitor to manufacture of medicine for prevention and/or treatment of fibrotic disease. Guangdong Zhongsheng Pharmaceutical Co., Ltd., Peop. Rep. China, 2017. p. 43pp.
- 14) Long C, Chen Z, Chen X, Zhang Y, Liu Z, Chen S, Li J. Crystal form and salt form of quinolinecarboxamide-thiourea and preparation method for tyrosine kinase inhibitor. Guangdong Zhongsheng Pharmaceutical Co., Ltd., Peop. Rep. China, 2018. p. 57pp.
- 15) LONG C, CHEN Z, CHEN X, ZHANG Y, LIU Z, LI P, CHEN S, LIANG G, XIE C, LI Z, FU Z, HU G, LI J. Triazinopy-rrole- and quinoline-urea derivatives as tyrosine kinase inhibitors and their preparation, pharmaceutical compositions and use in the treatment of cancer. Guangdong Zhongsheng Pharmaceutical Co., Ltd., Peop. Rep. China, 2016. p. 324pp.
- 16) LIU S, JING L, YU ZJ, WU C, ZHENG Y, ZHANG E, CHEN Q, YU Y, GUO L, WU Y, LI GB. ((S)-3-Mercapto-2-methylpropanamido)acetic acid derivatives as metallo-beta-lactamase inhibitors: Synthesis, kinetic and crystallographic studies. Eur J Med Chem 2018; 145: 649-660.
- 17) SHAN H, LI X, XIAO X, DAI Y, HUANG J, SONG J, LIU M, YANG L, LEI H, TONG Y, ZHOU L, XU H, WU Y. USP7

- deubiquitinates and stabilizes NOTCH1 in T-cell acute lymphoblastic leukemia. Signal Transduct Target Ther 2018; 3: 29.
- 18) Lai Q, Wang Y, Wang R, Lai W, Tang L, Tao Y, Liu Y, ZHANG R, HUANG L, XIANG H, ZENG S, GOU L, CHEN H, YAO Y, YANG J. Design, synthesis and biological evaluation of a novel tubulin inhibitor 7a3 targeting the colchicine binding site. Eur J Med Chem 2018; 156: 162-179.
- 19) Wei X, Zhang T, Yao Y, Zeng S, Li M, Xiang H, Zhao C, Cao G, Li M, Wan R, Yang P, Yang J. Efficacy of Lenvatinib, a multitargeted tyrosine kinase inhibitor, on laser-induced CNV mouse model of neovascular AMD. Exp Eye Res 2018; 168:
- 20) GUAN PP, DING WY, WANG P. The roles of prostaglandin F2 in regulating the expression of matrix metalloproteinase-12 via an insulin growth factor-2-dependent mechanism in sheared chondrocytes. Signal Transduct Target Ther 2018; 3: 27.
- 21) HAMANAKA RB, NIGDELIOGLU R, MELITON AY, TIAN Y, WITT LJ, O'LEARY E, SUN KA, WOODS PS, WU D,

- ANSBRO B, ARD S, ROHDE JM, DULIN NO, GUZY RD, MUTLU GM. Inhibition of phosphoglycerate dehydrogenase attenuates bleomycin-induced pulmonary fibrosis. Am J Respir Cell Mol Biol 2018; 58: 585-593.
- 22) Wollin L, Maillet I, Quesniaux V, Holweg A, Ryffel B. Antifibrotic and anti-inflammatory activity of the tyrosine kinase inhibitor Nintedanib in experimental models of lung fibrosis. J Pharmacol Exp Ther 2014; 349: 209-220.
- 23) ASHCROFT T, SIMPSON JM, TIMBRELL V. Simple method of estimating severity of pulmonary fibrosis on a numerical scale. J Clin Pathol 1988; 41: 467-470.
- 24) Nan J, Zhongyan Z. Bone marrow mesenchymal stem cells inhibited bleomycin-induced lung fibrosis. RSC Adv 2017; 7: 49498-49504. 25) Tatler AL, Jenkins G. TGF-beta activation and lung
- fibrosis. Proc Am Thorac Soc 2012; 9: 130-136.
- 26) RIES C. Cytokine functions of TIMP-1. Cell Mol Life Sci 2014; 71: 659-672.
- 27) GRUNWALD B, SCHOEPS B, KRUGER A. Recognizing the molecular multifunctionality and interactome of TIMP-1. Trends Cell Biol 2019; 29: 6-19.